Pergamon

Int. J. Solids Structures Vol. 32, No. 14, pp. 2053–2062, 1995
Elsevier Science Ltd
Printed in Great Britain

0020–7683(94)00218–5

ANALYSIS OF PIN-LOADED HOLES IN COMPOSITE LAMINATES UNDER COMBINED BEARING-BYPASS AND SHEAR LOADING

E. MADENCI and L. ILERI
Department of Aerospace and Mechanical Engineering, The University of Arizona, Tucson, AZ 85721, U.S.A.

and

J. H. STARNES, Jr
NASA Langley Research Center, Hampton, VA 23665, U.S.A.

(*Received* 4 *February* 1994; *in revised form* 25 *August* 1994)

Abstract—This study investigates the contact stresses in single-fastener mechanical joints in composite laminates with finite boundaries subjected to combined bearing-bypass and shear loading. The bearing stresses and the contact region are determined by imposing the appropriate mixed boundary conditions along the boundary of the hole. No-slip and slip zones of the contact region arising from the presence of friction are obtained as part of the analysis. A boundary collocation method, in conjunction with a complex variable formulation of the solution for anisotropic laminates, is utilized in the analysis.

INTRODUCTION

Bolts and rivets are used extensively in the construction of aircraft for transferring load among the structural components. The structural failure of these components usually begins at the fastener sites because high stress concentrations during take-off and landing render the fastener holes more susceptible to crack initiation. These cracks represent the most common origin of structural failures in aircraft. Therefore, accurate assessment of the contact stresses in mechanically fastened joints under general loading conditions is essential for reliable strength evaluation and failure prediction.

As the fastener transfers the load through the hole boundary, contact stresses develop over the contact region, neither of which is known *a priori*. In addition, the presence of material anisotropy, friction between the pin and the laminate, pin-hole clearance, combined bearing-bypass and shear loading, and finite geometry of the laminate result in a complex nonlinear problem.

Previous research concerning the analysis of mechanical joints subjected to combined bearing-bypass and shear loading is nonexistent. For the case of bearing-bypass loading only, Ramkumar (1981), Soni (1981) and Garbo and Ogonowski (1981) used the concept of superposition, which is not valid for nonlinear problems. Naik and Crews (1991) applied a linear finite element analysis, with conditions along the pin-hole contact region specified as displacement constraint equations based on the variation of the contact region as a function of the load. However, this variation is not known *a priori*. Also, their analysis is limited to symmetric geometry and material systems and to frictionless boundary conditions. Since the contact stress distribution and the contact region are not known *a priori*, they did not directly impose the boundary conditions appropriate for modeling the contact and non-contact regions between the fastener and the hole. Furthermore, finite element analysis is not suitable for iterative design calculations for optimizing laminate construction in the presence of fasteners under complex loading conditions. In this study, the solution method developed by Madenci and Ileri (1993) has been extended to determine

the contact stresses in single-fastener mechanical joints under combined bearing-bypass and shear loading.

PROBLEM STATEMENT

The geometry of the mechanical joint before and after applying combined bearing-bypass and shear loading is described in Fig. 1. Cartesian (x, y) and polar (r, θ) coordinate systems are employed, with their origins at the center of the pin-loaded hole. The hole and pin radii are denoted by a and R, respectively. The pin-hole clearance is specified by λ. The length and width of the finite rectangular region are denoted by L and H, respectively. The position of the pin in relation to the boundaries of the finite region is specified by l and h.

The composite laminates are composed of homogeneous, elastic, and orthotropic laminae, resulting in an anisotropic and homogeneous laminate with compliance coefficients, a_{ij}. Each lamina has material properties of elastic moduli, E_L and E_T; shear modulus, G_{LT}; and Poisson's ratio, ν_{LT}. The subscripts L and T denote the longitudinal and transverse directions relative to the fibers in the lamina.

The boundary conditions along the hole boundary are expressed as

$$u_r(a,\theta) = -(\delta_x \cos\theta + \delta_y \sin\theta - \lambda) \quad \theta \in [-\psi_2, \eta_2] \tag{1a}$$

$$u_\theta(a,\theta) = -(\delta_x \sin\theta - \delta_y \cos\theta) \quad \theta \in [-\psi_1, \eta_1] \tag{1b}$$

$$\sigma_{r\theta}(a,\theta) = \not{f}|\sigma_{rr}(a,\theta)| \quad \theta \in [\eta_1, \eta_2] \text{ and } \theta \in [-\psi_1, -\psi_2] \tag{1c}$$

$$\sigma_{rr}(a,\theta) = \sigma_{r\theta}(a,\theta) = 0 \quad \theta \in [\eta_2, -\psi_2] \tag{1d}$$

where u_r and u_θ are the displacement components and σ_{rr}, $\sigma_{\theta\theta}$, and $\sigma_{r\theta}$ are the stress components, all referenced to the polar coordinate system. The shear stress in the slip zone is determined by adopting a Coulomb friction model with coefficient of friction $\not{f}$. The components of the pin displacement in the x- and y-directions are denoted by δ_x and δ_y,

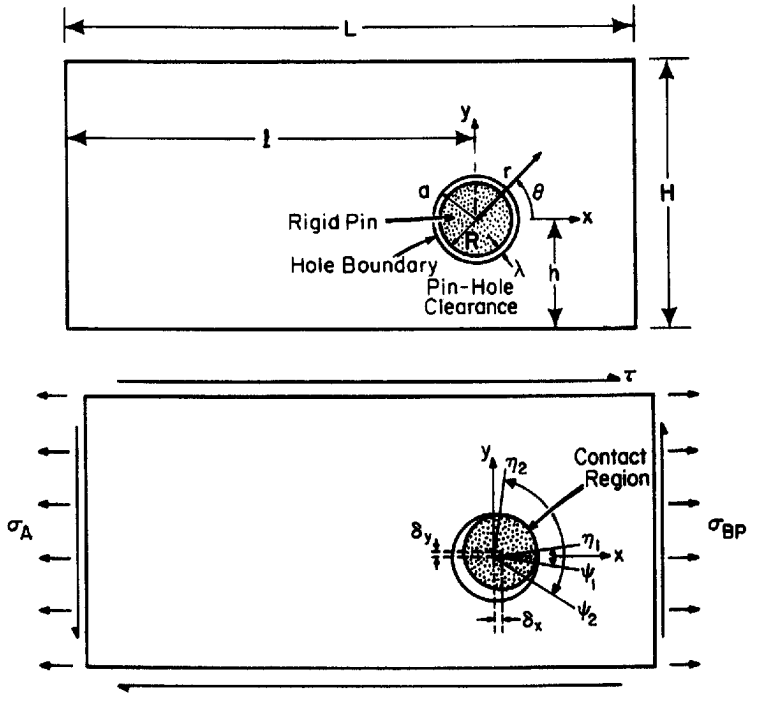

Fig. 1. Pin-loaded hole in a composite laminate before and after loading.

respectively. The angles η_1 and ψ_1 and η_2 and ψ_2 define the extent of the no-slip and slip zones and are determined as part of the solution by imposing the following constraints:

$$a\int_0^{2\pi} [-\sigma_{rr}(a,\theta)\cos\theta+\sigma_{r\theta}(a,\theta)\sin\theta]\,d\theta+(\sigma_{BP}-\sigma_A)H=0 \tag{2a}$$

$$a\int_0^{2\pi} [-\sigma_{rr}(a,\theta)\sin\theta+\sigma_{r\theta}(a,\theta)\cos\theta]\,d\theta=0 \tag{2b}$$

$$\sigma_{rr}(a,\theta)<0 \quad \theta\in[-\psi_2,\eta_2] \tag{2c}$$

$$\sigma_{rr}(a,-\psi_2)=\sigma_{rr}(a,\eta_2)=0 \tag{2d}$$

$$|\sigma_{r\theta}(a,\eta_1^-)-\sigma_{r\theta}(a,\eta_1^+)|=0 \tag{2e}$$

$$|\sigma_{r\theta}(a,-\psi_1^-)-\sigma_{r\theta}(a,-\psi_1^+)|=0. \tag{2f}$$

The superscripts $-$ and $+$ denote the angles associated with the no-slip and slip zones, respectively. The applied normal stresses are specified by σ_A and σ_{BP}, and the shear stress by τ. Enforcing the boundary conditions and the additional constraints results in a nonlinear load transfer problem. Therefore, determination of the contact stresses and the no-slip and slip zones of the contact region requires an iterative solution method.

SOLUTION METHOD

Utilizing the complex potential theory, Lekhnitskii (1968) introduced a solution method for the governing equations of two-dimensional elasticity concerning anisotropic laminates. He derived the expressions for the stress and displacement components in Cartesian coordinates as

$$\sigma_{xx}=2\,\mathrm{Re}\,[\mu_1^2\phi_1'(z_1)+\mu_2^2\phi_2'(z_2)] \tag{3a}$$

$$\sigma_{yy}=2\,\mathrm{Re}\,[\phi_1'(z_1)+\phi_2'(z_2)] \tag{3b}$$

$$\sigma_{xy}=-2\,\mathrm{Re}\,[\mu_1\phi_1'(z_1)+\mu_2\phi_2'(z_2)] \tag{3c}$$

$$u_x=2\,\mathrm{Re}\,[p_1\phi_1(z_1)+p_2\phi_2(z_2)]-\omega y+u_x^0 \tag{3d}$$

$$u_y=2\,\mathrm{Re}\,[q_1\phi_1(z_1)+q_2\phi(z_2)]-\omega y+u_y^0 \tag{3e}$$

where $\phi_1(z_1)$ and $\phi_2(z_2)$ are analytic functions and a prime denotes differentiation with respect to the corresponding argument. The complex variables z_1 and z_2 are defined by $z_k=x+\mu_k y$ with $k=1, 2$. The complex parameters μ_1 and μ_2 are the roots of the characteristic equation derived by Lekhnitskii,

$$a_{11}\mu^4-2a_{16}\mu^3+(2a_{12}+a_{66})\mu^2-2a_{66}\mu+a_{22}=0 \tag{4}$$

in which a_{ij} $(i,j=1,2,\ldots,6)$ are the compliance coefficients of the laminate. The parameters p_k and q_k are dependent on these coefficients and are given by $p_k=a_{11}\mu_k^2+a_{12}-a_{16}\mu_k$ and $q_k=a_{12}\mu_k+a_{22}/\mu_k-a_{26}$. In eqn (3), u_x^0 and u_y^0 represent the rigid-body displacements and ω, the rotations.

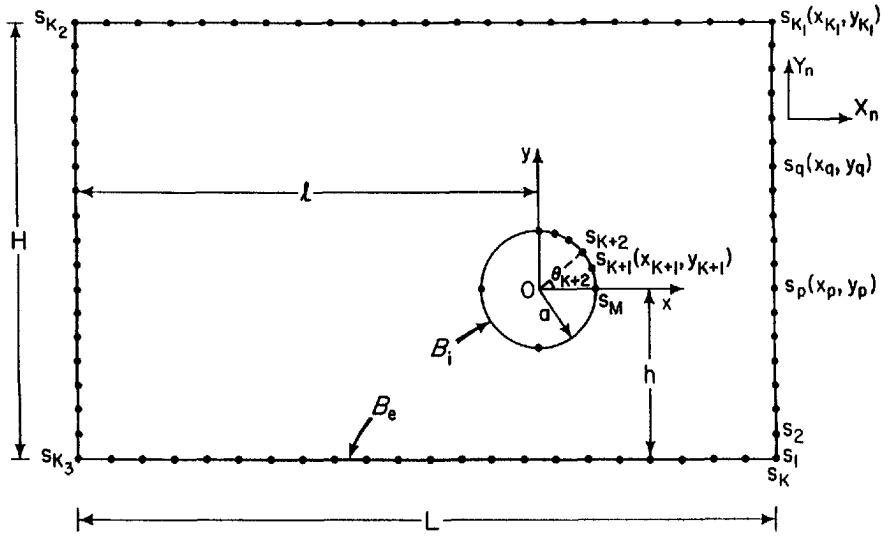

Fig. 2. Collocation points along the exterior and interior boundaries of the composite laminate.

The analytic functions $\phi_1(z_1)$ and $\phi_2(z_2)$ are expressed in the series form in terms of the mapping functions ξ_1 and ξ_2 as

$$\phi_1(\xi_1) = \alpha_0 \ln \xi_1 + \sum_{n=1}^{N} (\alpha_{-n}\xi_1^{-n} + \alpha_n \xi_1^n) \tag{5a}$$

$$\phi_2(\xi_2) = \beta_0 \ln \xi_2 + \sum_{n=1}^{N} (\beta_{-n}\xi_2^{-n} + \beta_n \xi_2^n). \tag{5b}$$

The mapping functions, ξ_1 and ξ_2, given by Lekhnitskii (1968) are

$$\xi_k = \frac{z_k \mp \sqrt{z_k^2 - a^2(1+\mu_k^2)}}{a(1-i\mu_k)} \quad k = 1, 2$$

in which $i = \sqrt{-1}$ and a is the radius of the hole.

The traction boundary conditions are imposed through resultant forces, $F_x(s)$ and $F_y(s)$, which are expressed in terms of the analytic functions as

$$\pm F_x(s) = 2\,\mathrm{Re}\,[\mu_1\phi_1(z_1) + \mu_2\phi_2(z_2)] - 2\,\mathrm{Re}\,[\mu_1\phi_1(z_1^p) + \mu_2\phi_2(z_2^p)] \tag{6a}$$

$$\mp F_y(s) = 2\,\mathrm{Re}\,[\phi_1(z_1) + \phi_2(z_2)] - 2\,\mathrm{Re}\,[\phi_1(z_1^p) + \phi_2(z_2^p)]. \tag{6b}$$

Upper and lower signs refer to the exterior, B_e, and interior, B_i, boundaries of the laminate. The complex variables $z_k^p = x_p + \mu_k y_p$ are associated with an arbitrary point on the boundary.

The unknown complex coefficients α_n and β_n are determined by imposing the boundary conditions at the collocation points, shown in Fig. 2, as well as the constraint equations and the requirement for single-valued displacement. The resulting over-determined system of algebraic equations in α_n, β_n are solved by the single-value decomposition method, resulting in explicit expressions for $\phi_1(z_1)$, $\phi_2(z_2)$, u_x, and u_y.

The boundary conditions associated with the collocation points are expressed as

$$F_x = \sigma_{BP} s_m \qquad F_y = \tau(s_m + h) \qquad m \in [1, K_1] \tag{7a}$$

$$F_x = \tau(s_m + l) \qquad F_y = 0 \qquad m \in [K_1 + 1, K_2] \tag{7b}$$

$$F_x = \sigma_A s_m \qquad F_y = \tau(s_m - H + h) \qquad m \in [K_2 + 1, K_3] \tag{7c}$$

$$F_x = \tau(s_m - L + l) \qquad F_y = 0 \qquad m \in [K_3 + 1, K] \tag{7d}$$

$$u_r(a, \theta_m) = -(\delta_x \cos\theta_m + \delta_y \sin\theta_m - \lambda) \qquad m \in [K+1, K_{\eta_2}] \tag{7e}$$

$$m \in [K_{\psi_2}, M]$$

$$u_\theta(a, \theta_m) = -(\delta_x \sin\theta_m - \delta_y \cos\theta_m) \qquad m \in [K+1, K_{\eta_1}] \tag{7f}$$

$$m \in [K_{\psi_1}, M]$$

$$\sigma_{r\theta}(a, \theta_m) = \not{f}|\sigma_{rr}(a, \theta_m)| \qquad m \in [K_{\eta_1} + 1, K_{\eta_2}] \tag{7g}$$

$$m \in [K_{\psi_2} + 1, M]$$

$$\sigma_{rr}(a, \theta_m) = 0 \qquad m \in [K_{\eta_2} + 1, K_{\psi_2} - 1] \tag{7h}$$

$$\sigma_{r\theta}(a, \theta_m) = 0 \qquad m \in [K_{\eta_2} + 1, K_{\psi_2} - 1]. \tag{7i}$$

In the discretized form, the constraint equations become

$$a \sum_{m=K+1}^{M} [-\sigma_{rr}(a, \theta_m)\cos\theta_m + \sigma_{r\theta}(a, \theta_m)\sin\theta_m]\Delta\theta_m + H(\sigma_{BP} - \sigma_A) = \varepsilon \tag{8a}$$

$$a \sum_{m=K+1}^{M} [-\sigma_{rr}(a, \theta_m)\sin\theta_m + \sigma_{r\theta}(a, \theta_m)\cos\theta_m]\Delta\theta_m = \varepsilon \tag{8b}$$

$$|\sigma_{rr}(a, \theta_{K_{\eta_2}})| = \varepsilon, \quad |\sigma_{rr}(a, \theta_{K_{\psi_2}})| = \varepsilon \tag{8c,d}$$

$$|\sigma_{r\theta}(a, \theta_{K_{\eta_1}} + 1) - \sigma_{r\theta}(a, \theta_{K_{\eta_1}})| = \varepsilon \tag{8e}$$

$$|\sigma_{r\theta}(a, \theta_{K_{\psi_1}} + 1) - \sigma_{r\theta}(a, \theta_{K_{\psi_1}})| = \varepsilon \tag{8f}$$

where ε is taken to be 10^{-5}. The position of the collocation points is denoted by s_m and θ_m along the exterior and interior boundaries, respectively; and the subscript m signifies the index of the collocation points. The numbering scheme for the collocation points is shown in Fig. 2, and certain indices are chosen as $K_1 = 101$, $K_2 = 163$, $K_3 = 265$, $K = 367$, and $M = 907$, based on a convergence study. The angle, $\Delta\theta_m$, between the two adjacent collocation points along the boundary of the hole varies based on their position specified by indices L_i ($i = 0, \ldots, 11$). Thus, the specific values for $\Delta\theta_m$ are defined as

$$\Delta\theta_m = \frac{\theta_{L_{i+1}} - \theta_{L_i}}{L_{i+1} - L_i} \quad m \in [L_{i+1}, L_i], \quad i = 0, \ldots, 11$$

where $L_0 = K+1$, $L_1 = K_{\eta_1} - 30$, $L_2 = K_{\eta_1} + 30$, $L_3 = K_{\eta_2} - 35$, $L_4 = K_{\eta_2} + 35$, $L_5 = K_{\eta_2} + 55$, $L_6 = K_{\psi_2} - 55$, $L_7 = K_{\psi_2} - 35$, $L_8 = K_{\psi_2} + 35$, $L_9 = K_{\psi_1} - 30$, $L_{10} = K_{\psi_1} + 30$, and $L_{11} = M$, with $L_1 - L_0 = 20$, $L_3 - L_2 = 50$, $L_6 - L_5 = 100$, $L_9 - L_8 = 50$, and $L_{11} - L_{10} = 20$. The indices associated with the angles specifying the no-slip, K_{η_1} and K_{ψ_1}, and slip, K_{η_2} and K_{ψ_2}, zones are determined as part of the solution.

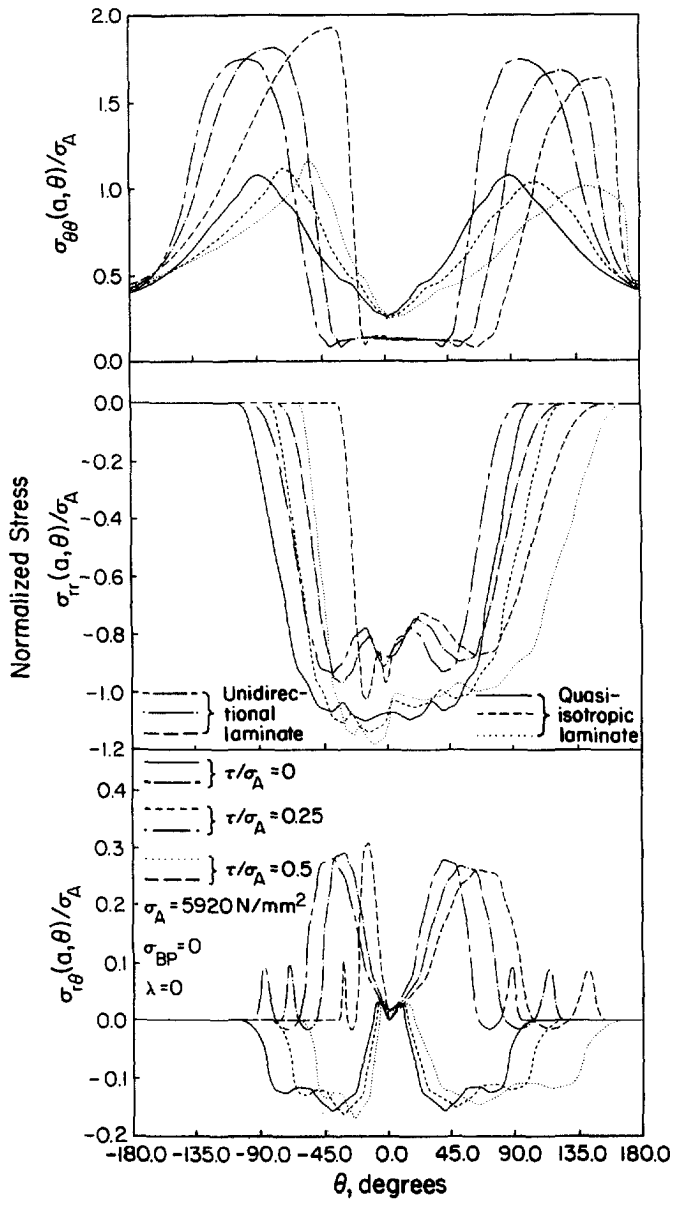

Fig. 3. The effect of shear loading on the stresses along the boundary of the pin-loaded hole for quasi-isotropic and unidirectional laminates in the absence of bypass loading.

NUMERICAL RESULTS

In order to illustrate the effect of material anisotropy on contact stresses, a quasi-isotropic $[(0_4^\circ/45_4^\circ/-45_4^\circ/90_4^\circ)_s]$ and a unidirectional laminate $[(0_{32}^\circ)]$ are considered in this study. The material properties and the geometry of the laminates are the same as those specified by Hyer and Liu (1984) in their experimental work concerning only the bearing load. The lamina properties are specified as $E_L = 37.2$ GPa, $E_T = 12.3$ GPa, $G_{LT} = 3.93$ GPa, and $\nu_{LT} = 0.3$. The coefficient of friction, f, is taken to be 0.2 throughout this study. The geometry of the laminates is prescribed by $a = 25.4$ mm, $L = 292$ mm, $H = 203$ mm, $l = 191$ mm, and $h = 101.5$ mm.

In the absence of bypass loading, the effect of shear loading on the contact stresses and the contact region is captured by considering a range of normalized applied shear loadings, τ/σ_A. The variation of the stresses along the boundary of the hole for the case of a snug fit ($\lambda = 0$) is presented in Fig. 3. The angles defining the no-slip and slip zones corresponding to these loading ratios and the components of the pin displacement are

Table 1. Pin displacement components and the angles specifying the extent of no-slip and slip zones in the contact region: $\sigma_A = 5920\ N/mm^2$, $\sigma_{BP} = 0$, *and* $\lambda = 0$

	Contact Angles (degrees)				Pin Displacement (mm)	
τ/σ_A	η_1	ψ_1	η_2	ψ_2	δ_x	δ_y
			Quasi-Isotropic Laminate			
0.00	4.650	−4.650	104.020	−104.020	0.009775	0.000000
0.25	4.840	−3.240	125.840	−84.240	0.006782	0.002567
0.50	6.480	−2.440	168.480	−63.440	0.003550	0.004765
			Unidirectional Laminate			
0.00	4.560	−4.560	96.090	−96.090	0.004225	0.000000
0.25	5.184	−3.216	124.416	−77.184	0.003851	0.002167
0.50	6.408	−1.504	153.792	−36.096	0.003020	0.004267

tabulated in Table 1. For the case of zero shear loading, the analytical predictions shown in Fig. 3 agree well with the experimental results given by Hyer and Liu (1984). In another study, Madenci and Ileri (1993) compared their analytical predictions with the experimental results reported by Hyer and Liu in the absence of bypass and shear loading. The presence of shear loading results in an increase of the peak values of tangential and shear stresses for both quasi-isotropic and unidirectional material systems. Figure 3 shows that these two laminate configurations have considerably different tangential and shear stress distributions along the boundary of the hole, even though they are subjected to the same loading conditions. The variation of the radial stresses, however, is not very sensitive. The locations signifying the peak values of the stresses vary significantly as a function of the applied shear load. Also, the asymmetric stress distributions become more pronounced for increasing applied shear load.

The variation of the stresses along the boundary of the hole in the presence of bypass loading for a normalized shear loading (τ/σ_A) of 0.25 is presented in Fig. 4. The magnitudes of the contact stresses decrease significantly for increasing normalized bypass loading for both material systems. However, the distribution of the stresses, specific to each material system, seems to have the same general trend. The angles prescribing the extent of the contact regions are provided in Table 2. The contact region becomes smaller as the bypass loading increases.

Under specific normalized shear (τ/σ_A) and bypass (σ_{BP}/σ_A) loading of 0.25, the influence of the clearance on the contact stresses is captured by considering 1% and 2.5% of the diameter of the pin-hole as clearances. A reduction in contact stresses with increasing clearance is observed in Fig. 5. The amount of clearance has a considerable effect on the peak values of all the stress components. The position of the no-slip and slip zones is dependent on the amount of clearance. The specific values for these angles are tabulated in Table 3. In the case of quasi-isotropic material, the extent of the total contact region is not very sensitive to the changes in clearance; however, the total contact region decreases for unidirectional material.

CONCLUSIONS

This study investigates the influence of combined bearing-bypass and shear loading on the contact stresses arising in pin-loaded holes in laminated composites. The analysis is capable of predicting the stresses and the contact region along the boundary of the hole by imposing the appropriate mixed boundary conditions. Also, it accounts for the effects of finite geometry, material anisotropy, and friction between the rigid pin and the laminate. Due to the lack of symmetry in loading, previous analyses could not consider combined bearing-bypass and shear loading. This is the first analytical study capable of including the effect of shear loading. This analysis provides an accurate capability for predicting the strength of the mechanical joint by employing certain failure criteria.

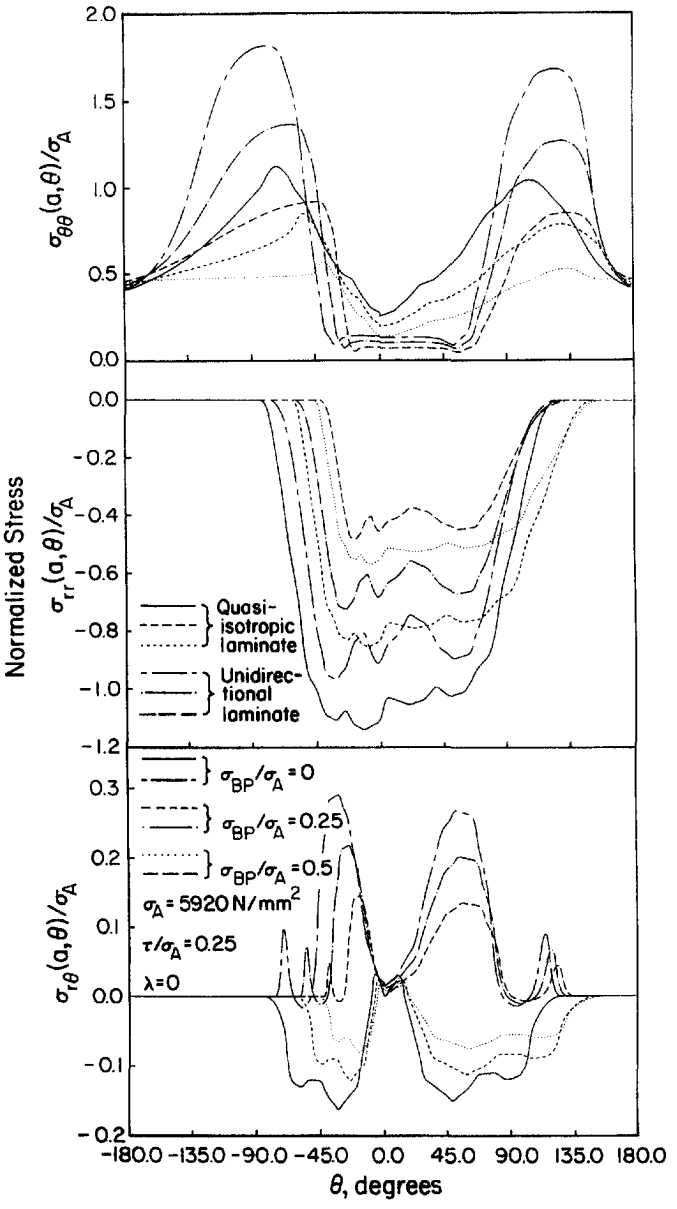

Fig. 4. The effect of bypass loading on the stresses along the boundary of the pin-loaded hole for quasi-isotropic and unidirectional laminates in the presence of shear loading.

Table 2. Pin displacement components and the angles specifying the extent of no-slip and slip zones in the contact region: $\sigma_A = 5920\ N/mm^2$, $\tau/\sigma_A = 0.25$, *and* $\lambda = 0$

	Contact Angles (degrees)				Pin Displacement (mm)	
σ_{BP}/σ_A	η_1	ψ_1	η_2	ψ_2	δ_x	δ_y
			Quasi-Isotropic Laminate			
0.00	4.840	−3.240	125.840	−84.240	0.006782	0.0025670
0.25	5.840	−2.400	151.840	−62.400	0.006975	0.0026110
0.50	6.040	−1.800	157.040	−46.800	0.007325	0.0026220
			Unidirectional Laminate			
0.00	5.184	−3.216	124.416	−77.184	0.003851	0.0021671
0.25	5.384	−2.500	129.216	−60.000	0.003571	0.0021685
0.50	5.580	−1.784	133.920	−42.816	0.003399	0.0021695

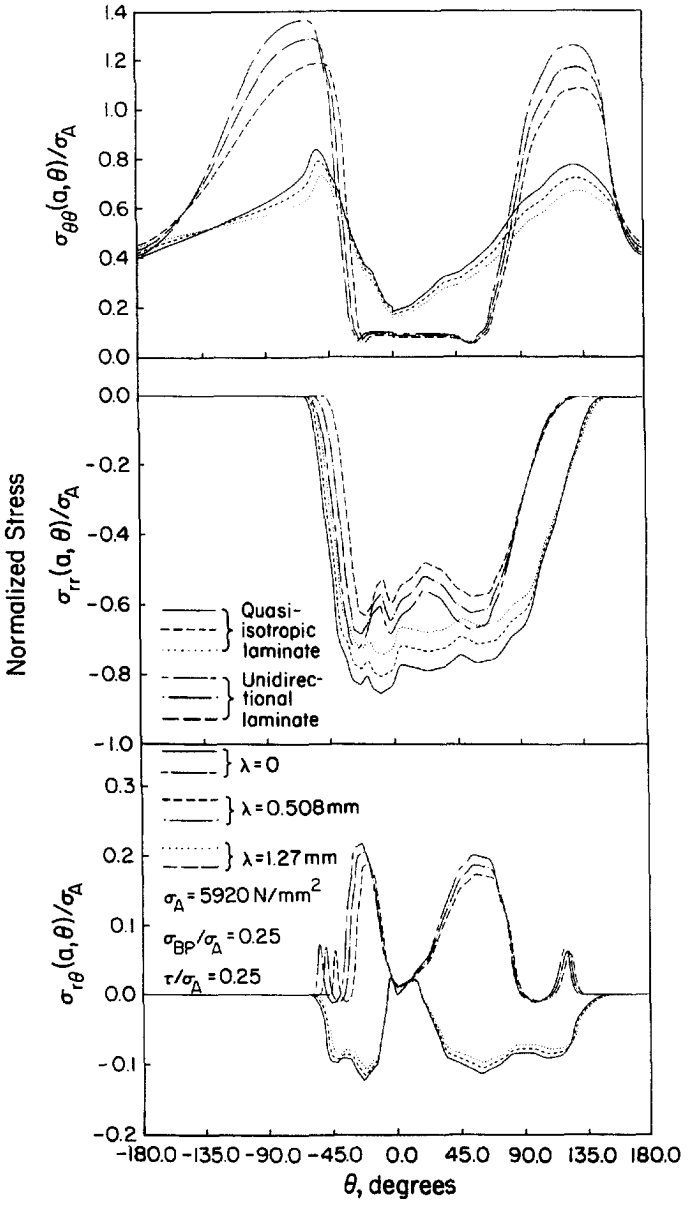

Fig. 5. The effect of clearance on the stresses along the boundary of the pin-loaded hole for quasi-isotropic and unidirectional laminates in the presence of both bypass and shear loading.

Table 3. Pin displacement components and the angles specifying the extent of no-slip and slip zones in the contact region : $\sigma_A = 5920\ N/mm^2$, $\sigma_{BP}/\sigma_A = 0.25$, *and* $\tau/\sigma_A = 0.25$

λ (mm)	Contact Angles (degrees)				Pin Displacement (mm)	
	η_1	ψ_1	η_2	ψ_2	δ_x	δ_y
			Quasi-Isotropic Laminate			
0.000	5.840	−2.400	151.840	−62.400	0.006975	0.0026112
0.508	5.920	−2.320	153.920	−60.320	0.006812	0.0021002
1.270	6.000	−2.240	156.000	−58.240	0.006715	0.0019871
			Unidirectional Laminate			
0.000	5.384	−2.500	129.216	−60.000	0.003571	0.0021685
0.508	5.460	−2.300	131.040	−55.200	0.003291	0.0021002
1.270	5.540	−2.000	132.960	−48.000	0.002812	0.0020012

Most existing analyses on mechanical joints are confined to single fasteners. Investigations using current analytical and numerical capabilities for determining the contact stresses among multi-fasteners do not exist in the literature. This method can be extended to eliminate this void while synthesizing all of the various effects, such as finite geometry, pin-hole clearance, presence of edge cracks, friction, bypass loading, and interactions among fasteners, into a comprehensive design/analysis methodology suitable for fast design iterations.

REFERENCES

Hyer, M. W. and Liu, D. (1984). Stresses in pin-loaded plates: photoelastic results. *J. Compos. Mater.* **19,** 138–153.

Garbo, S. P. and Ogonowski, J. M. (1981). Effect of variances and manufacturing tolerances on the design strength and life of mechanically fastened composite joints. *Methodology Development and Data Evaluation*, Vol. 1–3, AFWAL-TR-3041.

Lekhnitskii, S. G. (1968). *Anisotropic Plates*. Gordon and Breach, New York.

Madenci, E. and Ileri, L. (1993). Analytical determination of contact stresses in mechanically fastened composite laminates with finite boundaries. *Int. J. Solids Structures* **30,** 2469–2484.

Naik, R. and Crews, J. H., Jr. (1991). Stress analysis method for clearance-fit joints with bearing-bypass loading. *AIAA J.* **29,** 89–95.

Ramkumar, R. L. (1981). Bolted joint design. In *Test Methods and Design Allowables for Fibrous Composites* (Edited by C. C. Chamis), pp. 376–395. ASTM STP 734, American Society for Testing and Materials, Philadelphia, Pennsylvania.

Soni, S. R. (1981). Stress and strength analysis of bolted joints in composite laminates. In *Composite Structures* (Edited by I. H. Marshall), pp. 50–62. Applied Science Publishers, London.